



Citation for published version:

Walsh, A 2011, 'Surface oxygen vacancy origin of electron accumulation in indium oxide', *Applied Physics Letters*, vol. 98, no. 26, 261910. <https://doi.org/10.1063/1.3604811>

DOI:

[10.1063/1.3604811](https://doi.org/10.1063/1.3604811)

Publication date:

2011

[Link to publication](#)

Copyright 2011 American Institute of Physics. This article may be downloaded for personal use only. Any other use requires prior permission of the author and the American Institute of Physics.

This article appeared in Walsh, A., 2011. Surface oxygen vacancy origin of electron accumulation in indium oxide. *Applied Physics Letters*, 98 (26), 261910 and may be found at <http://dx.doi.org/10.1063/1.3604811>

University of Bath

Alternative formats

If you require this document in an alternative format, please contact:
openaccess@bath.ac.uk

General rights

Copyright and moral rights for the publications made accessible in the public portal are retained by the authors and/or other copyright owners and it is a condition of accessing publications that users recognise and abide by the legal requirements associated with these rights.

Take down policy

If you believe that this document breaches copyright please contact us providing details, and we will remove access to the work immediately and investigate your claim.

Surface oxygen vacancy origin of electron accumulation in indium oxide

Aron Walsh^{a)}

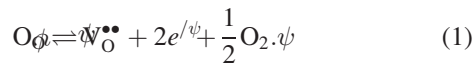
Centre for Sustainable Chemical Technologies and Department of Chemistry, University of Bath, Claverton Down, Bath BA2 7AY, United Kingdom

(Received 18 April 2011; accepted 7 June 2011; published online 29 June 2011)

Metal oxides are typically insulating materials that can be made conductive through aliovalent doping and/or non-stoichiometry. Recent studies have identified conductive states at surfaces and interfaces of pure oxide materials; high electron concentrations are present, resulting in a high-mobility two-dimensional electron gas. We demonstrate for In_2O_3 that the energy required to form an oxygen vacancy decreases rapidly towards the (111) surface, where the coordination environment is lowered. This is a general feature of metal oxide systems that can result in a metal–insulator transition where donors are produced at chemically reduced extended defects.

© 2011 American Institute of Physics. [doi:10.1063/1.3604811]

Metal oxide based electronics is an active field of research,¹ which has led to the recent discovery of a high-mobility electron gas at material interfaces and surfaces.^{2–4} This phenomenon, which gives rise to metallic conduction in formally insulating materials, has been found at the interface of perovskite ternary oxides² as well as the surfaces of In_2O_3 ,⁴ CdO ,⁵ and SrTiO_3 .⁶ The cause has been attributed to a combination of electrical dipoles and lattice defects,⁷ e.g., the formation of an oxygen vacancy defect can donate two electrons to the lattice



What is the microscopic origin of these effects? In this letter, we answer this question using a combination of first-principles and electrostatic techniques applied to the surface of In_2O_3 ; we observe a rapid decrease in the formation energy for oxygen vacancies towards the material surface, which correlates directly with the change in Madelung site potential of the oxide ions. The change is sufficient to induce a metal–insulator transition at the material surface.

The surface structure of indium oxide was recently addressed in a combined experimental and computational investigation:⁸ the (111) terminated structure is lowest in energy and therefore the most abundant crystal face in thermodynamic equilibrium. We adopt the same model of the (111) terminated non-polar surface, consisting of 240 atoms in the periodically repeating unit.⁹ We have modelled the formation of oxygen vacancies on this surface using two methodologies. First, we employ a quantum mechanical (QM) approach based on density functional theory, as implemented in the all-electron, numerical basis code *FHI-AIMS*.¹⁰ Scalar-relativistic effects were treated within the scaled ZORA approximation,¹¹ and exchange-correlation effects are treated at the PBEsol level.¹² All defect calculations were performed in a neutral charge state, which avoids the issue of partially screened electrostatic interactions, as well as energy corrections associated with image charges on a dielectric surface.¹³ Second, we employ a classical treatment based on a polarisable interatomic

potential (IP) model derived for In_2O_3 ,¹⁴ which we have implemented in the code *GULP*.¹⁵

The structural model consists of a 2 nm slab of In_2O_3 . The energy for oxygen removal, as defined in Eq. (1), was assessed for each of the symmetry inequivalent oxygen sites. The results are shown in Fig. 1 for the QM approach; in the centre of the slab, the formation energy approaches 2 eV, which is the value calculated at infinite dilution in the bulk material. Approaching the surface, there is a rapid decrease of the formation energy to more than 50% of the initial value (a decrease to 0.95 eV). The concentration gradient of oxygen donor defects is also shown in Fig. 1, which has been calculated assuming a Boltzmann distribution of the non-interacting point defects at a temperature of 750 K.¹⁶

A disperse conduction band is formed for the (111) surface,⁹ which is similar to the bulk of In_2O_3 . Crucially for conductivity, the occupied donor levels produced by the surface oxygen vacancies are spatially delocalised, as shown in Fig. 2, in contrast to the bulk material;¹⁷ this is directly related to the reduced electrostatic site potential to be described below. We can consider the defect concentration necessary to induce metallic conduction at the oxide surface. For electron impurities, the metal–insulator transition will occur when the carrier concentration (n) exceeds the Mott criterion^{18,19}

$$n^{-\frac{1}{3}} > \sqrt[3]{2.6} a_0 \cdot \psi \quad (2)$$

where a_0 is the effective Bohr radius of the conduction electron

$$a_0 = \frac{4\pi\epsilon_s\hbar^2}{m^*e^2} \cdot \psi \quad (3)$$

Within effective mass theory, taking the static dielectric constant (ϵ_s) of $10 \epsilon_0$ and an isotropic electron mass (m^*) of $0.3 m_e$ results in an effective Bohr radius of 1.8 nm for In_2O_3 ; the electron wavefunction extends over 64 unit cells. A critical carrier concentration of $1 \times 10^{19} \text{ cm}^{-3}$ is therefore expected, which corresponds to a sheet density of $5 \times 10^{12} \text{ cm}^{-2}$. An accumulation layer of $7.2 \times 10^{12} \text{ cm}^{-2}$ has been reported by King *et al.*⁴ for thin-film In_2O_3 , which is above the Mott criterion, and corresponds to approximately one ionised surface vacancy per four $\sqrt{2}a \times \sqrt{2}a \times \frac{\sqrt{3}}{2}$ surface

^{a)}Electronic mail: a.walsh@bath.ac.uk.

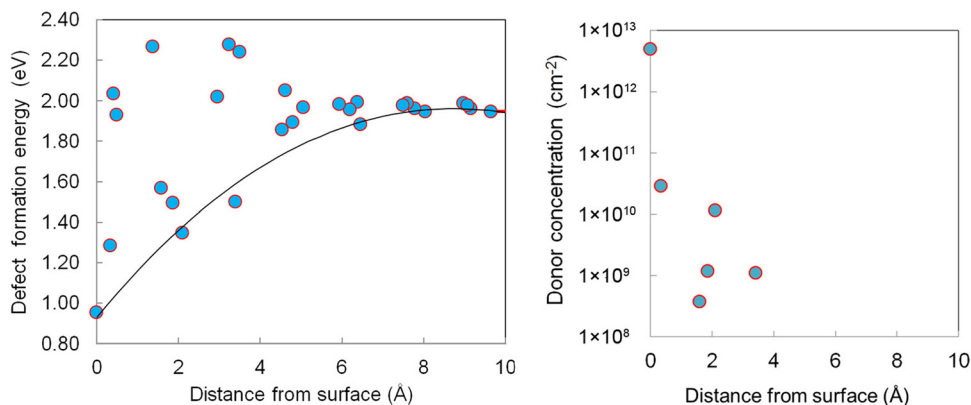


FIG. 1. (Color online) (left panel) Energy of formation for an oxygen vacancy in In_2O_3 as a function of distance from the (111) terminated surface, as calculated by density functional theory. (right panel) Distribution of surface donors at an equilibrium temperature of 750 K (Ref. 16).

cells (where a represents the cubic lattice constant of 1.012 nm). Given the calculated defect formation energies, this level of non-stoichiometry is achievable at high temperatures and/or low oxygen partial pressures and will arise primarily from vacancies created at the topmost oxygen layer, as shown in Fig. 1.

Explicit calculation of the surface defect structure is a computationally demanding process. To judge the applicability of a technique more accessible for complex or disordered systems, we have also calculated the local Madelung (electrostatic) site potentials for each of the oxygen sites in the 2 nm slab, defined as

$$M_O = \frac{e}{4\pi\epsilon_0} \sum_{ions} \frac{q_{ion}}{r_{O-ion}} \cdot \psi \quad (4)$$

In the bulk bixbyite lattice, all oxygen sites are equivalent by symmetry (the $48e$ Wyckoff position), and the site potential is calculated to be 22.92 V.¹⁴ For the topmost surface site, the oxygen coordination number is lowered from 4 to 3 and there is a corresponding decrease of 0.8 V in the electrostatic potential. The potential does not decrease monotonically towards the surface; the same fluctuations are observed as for the defect formation energies (Fig. 1).

The origin of the fluctuations in the oxygen removal energy (potential distribution) is evident from an analysis of

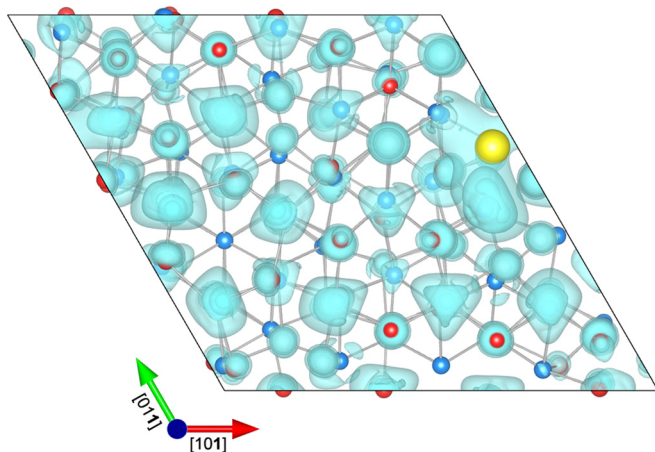


FIG. 2. (Color online) Electron density associated the occupied defect state for the lowest energy oxygen vacancy ($O1$ site) on the (111) surface of In_2O_3 . The indium atoms are coloured blue (dark gray), with red (light gray) reserved for oxygen. The vacancy site is filled with a large ball, and the electron density isosurface is shaded; the charge is highly delocalised, which is characteristic of a shallow defect centre.

the upper surface structure shown in Fig. 3. One factor influencing the removal energy is the coordination number (a decrease in coordination from the bulk value results in a lower cost for removal), while the second is the coordination of the nearest neighbour indium atoms (the cost of breaking a bond with a highly coordinated indium atom is lower). The combination of these changes results in $O1$ having a formation energy substantially lower than the bulk value and $O5$ having a value higher than the bulk value. The resulting oscillations are present until almost 6 Å into the surface, which are related to the complex bixbyite (defective fluorite) crystal structure of In_2O_3 . The decrease in site potential will also disfavour the trapping of electrons at the vacancy sites, i.e., the colour-centre that has been calculated for the bulk material.¹⁷

The phenomenon of surface stabilised defect reactions is not unknown. For example, Duffy *et al.*¹³ studied the formation of oxygen vacancies on the stable non-polar (001) surface of MgO ; the defect formation energy decreased by 0.16 eV towards the surface. The (001) rocksalt surface represents an upper limit in terms of a close-packed, high coordination surface termination, which means that 0.16 eV should be the lower bound for a decrease in the oxygen removal energy.

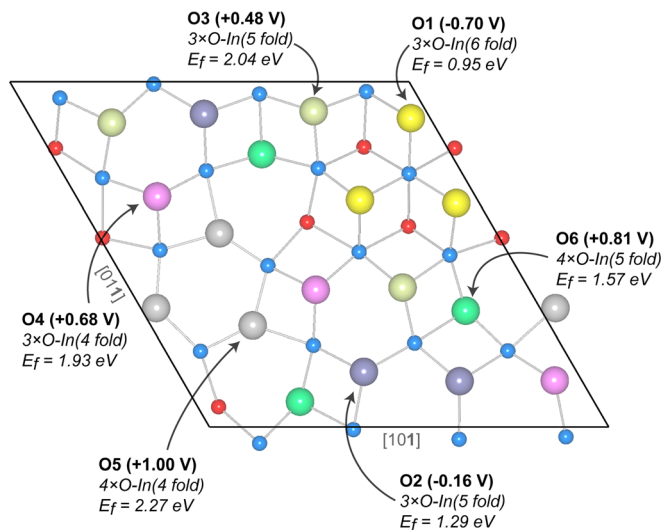


FIG. 3. (Color online) The upper surface structure of (111) terminated In_2O_3 . The first 6 inequivalent oxygens are labelled numerically from the topmost atom; with threefold rotational symmetry, these account for the first 18 oxygen atoms. The local site potential, coordination with respect to indium (with the lowest indium coordination in parenthesis) and the oxygen removal energy (E_f) are listed for each site.

For a dioxide, less ideal surface terminations occur; the distribution of oxygen site potentials for the surfaces of rutile and anatase TiO₂ have been reported by Woning and Van Santen,²⁰ where the fluctuations are of the order of 2.3 V for (001) rutile, compared to the (110) rutile (0.5 V) and (001) anatase (2.4 V) faces. Combined with changes in the cation potential, the greater reducibility of the rutile polymorph was explained. For CeO₂ nanoparticles, Migani *et al.*²¹ reported a similar effect, where the reduced electrostatic potential was calculated for low coordination surface sites along with a linear dependence on the oxygen removal energy, which can vary by over 2 eV; the same effect has been reported for thin-films of ceria.^{22,23} However, in order to obtain high conductivity, the combination of the reduced donor formation energy with a large effective Bohr radius is required.

In conclusion, a metal–insulator transition is achievable on indium oxide surfaces through oxygen loss due to the drastic lowering of defect reaction energy and the creation of delocalised donor states. Given the exponential dependence of the concentration of oxygen vacancy defects with the reaction energy, even small variations can be critical in determining electron carrier concentrations under equilibrium conditions. The same variations in site potentials will occur at material interfaces and indeed grain boundaries and dislocations. This suggests that more complex material systems and phenomena can be rationalised through electrostatic models, which may not require explicit electronic structure calculations. Finally, our results demonstrate that the extended defects present a potential route to overcoming the doping limits^{24–26} established for bulk semiconducting and wide band-gap materials.

I would like to acknowledge useful discussions with P. D. C. King, C. R. A. Catlow, and A. A. Sokol. Access to the HECToR supercomputer was facilitated through membership of the UK's HPC Materials Chemistry Consortium, which is funded by EPSRC (Grant No. EP/F067496).

- ¹J. Mannhart and D. Schlom, *Science* **327**, 1607 (2010).
- ²H. Hwang, *Science* **313**, 1895 (2006).
- ³A. Santander-Syro, O. Copie, T. Kondo, F. Fortuna, S. Pailhes, R. Weht, X. Qiu, F. Bertran, A. Nicolaou, and A. Taleb-Ibrahimi, *Nature* **469**, 189 (2011).
- ⁴P. D. C. King, T. D. Veal, D. J. Payne, A. Bourlange, R. G. Egdell, and C. F. McConville, *Phys. Rev. Lett.* **101**, 116808 (2008).
- ⁵P. D. C. King, T. D. Veal, C. F. McConville, J. Zúñiga Pérez, V. Muñoz Sanjosé, M. Hopkinson, E. D. L. Rienks, M. F. Jensen, and P. Hofmann, *Phys. Rev. Lett.* **104**, 256803 (2010).
- ⁶W. Meevasana, P. D. C. King, R. H. He, S.-K. Mo, M. Hasimoto, A. Tamai, P. Songsiririthigul, F. Baumberger, and Z.-X. Shen, *Nat. Mater.* **10**, 114 (2011).
- ⁷E. Dagotto, *Nature* **469**, 167 (2011).
- ⁸K. H. L. Zhang, A. Walsh, C. R. A. Catlow, V. K. Lazarov, and R. G. Egdell, *Nano Lett.* **79**, 3740 (2010).
- ⁹A. Walsh and C. R. A. Catlow, *J. Mater. Chem.* **20**, 10438 (2010).
- ¹⁰V. Blum, R. Gehrke, F. Hanke, P. Havu, V. Havu, X. Ren, K. Reuter, and M. Scheffler, *Comput. Phys. Commun.* **180**, 2175 (2009).
- ¹¹E. van Lenthe, E. J. Baerends, and J. G. Snijders, *J. Chem. Phys.* **101**, 9783 (1994).
- ¹²J. P. Perdew, A. Ruzsinszky, G. I. Csonka, O. A. Vydrov, G. E. Scuseria, L. A. Constantin, X. Zhou, and K. Burke, *Phys. Rev. Lett.* **100**, 136406 (2008).
- ¹³D. M. Duffy, J. P. Hoare, and P. W. Tasker, *J. Phys. C* **17**, 195 (1983).
- ¹⁴A. Walsh, C. R. A. Catlow, A. A. Sokol, and S. M. Woodley, *Chem. Mater.* **21**, 4962 (2009).
- ¹⁵J. D. Gale and A. L. Rohl, *Mol. Simul.* **29**, 291 (2003).
- ¹⁶A sheet donor density of $5 \times 10^{12} \text{ cm}^{-2}$ is distributed across the surface based on the calculated vacancy formation energies and $T = 750 \text{ K}$. A rigorous approach requires temperature dependent defect free energies, which would enable quantitative predictions of equilibrium constants.
- ¹⁷S. Lany and A. Zunger, *Phys. Rev. Lett.* **106**, 069601 (2011).
- ¹⁸N. F. Mott, *Rev. Mod. Phys.* **40**, 677 (1968).
- ¹⁹P. P. Edwards and M. J. Sienko, *Phys. Rev. B* **17**, 2575 (1978).
- ²⁰J. Woning and R. A. Van Santen, *Chem. Phys. Lett.* **101**, 541 (1983).
- ²¹A. Migani, G. N. Vayssilov, S. T. Bromley, F. Illas, and K. M. Neyman, *J. Mater. Chem.* **20**, 10535 (2010).
- ²²X. T. Sayle, S. C. Parker, and C. R. A. Catlow, *J. Chem. Soc., Chem. Commun.* **1992**, 977 (1992).
- ²³M. Nolan, J. E. Fearon, and G. W. Watson, *Solid State Ionics* **177**, 3069 (2006).
- ²⁴C. R. A. Catlow, A. A. Sokol, and A. Walsh, *Chem. Commun.* **47**, 3386 (2011).
- ²⁵W. Walukiewicz, *Physica B* **302–303**, 123 (2001).
- ²⁶S. B. Zhang, S.-H. Wei, and A. Zunger, *Phys. Rev. Lett.* **84**, 1232 (2000).